

Remote Sensing Fire and Fuels in Southern California

Philip J. Riggan^A
Lynn G. Wolden^A
Robert G. Tissell^A
David R. Weise^A
Janice Coen^B

^AUSDA Forest Service, Pacific Southwest Research Station, 4955 Canyon Crest Drive,
Riverside, CA 92507 USA, priggan@fs.fed.us.

^BNational Center for Atmospheric Research, P.O. Box 3000, Boulder, CO 80301 USA.

Abstract: Airborne remote sensing at infrared wavelengths has the potential to quantify large-fire properties related to energy release or intensity, residence time, fuel-consumption rate, rate of spread, and soil heating. Remote sensing at a high temporal rate can track fire-line outbreaks and acceleration and spotting ahead of a fire front. Yet infrared imagers and imaging spectrometers typically used for earth remote sensing are saturated by—and incapable of measuring—the very bright infrared light that radiates from wildland fires.

The Forest Service, Pacific Southwest Research Station, and its partners have addressed this problem by developing the FireMapper thermal-imaging radiometer for quantitative, high-resolution measurements of wildland fires. FireMapper has been applied to produce and disseminate accurate visualizations of large-fire activity, during active burning periods and for multiple fires, in near real-time.

Practical extension of measurements by the FireMapper to prediction of fire behavior on time scales from hours to days requires highly resolved information on fuels and wind across landscapes and changes to the basic Rothermel formulation for fire spread. Combined sampling in the field and by multispectral remote sensing for the 2006 Esperanza Fire have demonstrated that the latter may provide an improved means for acquiring the needed fuels data.

Additional Keywords: chaparral, Esperanza Fire, FireMapper

Introduction

Very large and destructive wildfires are becoming common in the Mediterranean-type ecosystems of coastal southern California. Of the ten largest fire complexes recorded there over nearly a century, seven have occurred since 2003 (data *available online*¹). Large-fire impacts on ecosystems and society have been high: more than 860,000 hectares have been burned, communities of 500,000 residents have been ordered evacuated, 9300 structures have been destroyed, and California mixed-conifer forest has been killed by crown fire with little or no subsequent regeneration in portions of San Diego, Los Angeles, and San Bernardino counties (data *available online*¹, Los Angeles Times 2007, Franklin *et al.* 2006). Absent adaptive changes in fire policy or management effectiveness, the trend might be expected to continue. Such adaptation will require timely fire intelligence data and more sophisticated fuel and fire behavior models to evaluate expected fire behavior in support of tactical fire suppression and decisions

¹ < http://fam.nwcg.gov/fam-web/hist_209/report_list_209>

regarding strategic management of fuels by prescribed burning or other means. In this paper we describe recent applications of airborne remote sensing for fire measurements and monitoring and the state of knowledge regarding chaparral fuel development as required for interpretation of those measurements and fire-behavior modeling.

Fire intelligence

Current knowledge of fire behavior in chaparral, which has been the plant community most involved in these large fires, is largely derived from simulation models and records of final fire location and area, from which have been derived fire-regime statistics involving distribution of fire size, season of occurrence, and frequency. Analyses of fire records lack specificity on fuel loading and fire behavior and do little to illuminate the forces behind an event. Operational fire-behavior simulation models and some research models are derived from the Rothermel model (Rothermel 1972), which was developed largely from laboratory-based measurements of fire spread in small, uniform fuel beds and a description of the effects of wind on fire spread in Australian grasslands. The applicability of the Rothermel model and its descendents to large-fire behavior in chaparral is uncertain, partly because of poor descriptions of extant fuels, non-linearity of scaling with fire size in the laboratory (cf, Fendell *et al.* 1990), order-of-magnitude extrapolations in energy release and rate of spread required to simulate large fires, inability to consider fire-atmosphere interactions, and the questionable application to live fuels of relationships based upon burning excelsior and pine needle beds. Most problematic for chaparral is the linkage of wind effects in the Rothermel model to the no-wind rate of spread, which in chaparral may be zero at higher fuel moistures and low dead-fuel loading. In the field, higher wind speeds may override these factors to produce substantial rates of fire spread even as the model must predict zero spread. Improvements in this prediction system clearly must come from measurements of real-world wildland fires at their full intensity and extent.

Fire intelligence regarding fire location and movement until recently has been derived largely from infrared line-scanner imagery collected in early evening, occasional mapping of a fire's perimeter based on the GPS-determined locations of a low-level helicopter flight along that perimeter, and ad hoc reports from ground- and aircraft-based observers. While these sources of information are valuable, especially on remote, slowly moving fires, they provide little information on current direction and rates of fire movement or homes and resources threatened during critical periods of fire activity, such as when the Cedar Fire burned into the City of San Diego, the Old Fire burned into San Bernardino, or the Jesusita or Tea fires burned into communities of Santa Barbara County. Similarly, traditional sources of fire intelligence provide little information of value in understanding fire behavior or effects or improving fire-suppression response.

The FireMapper thermal-imaging radiometer

The USDA Forest Service, Pacific Southwest Research Station (PSW), and its partners have developed and are applying new airborne remote-sensing technology to measure and understand wildfire behavior and impacts in the environment (Riggan and Tissell 2009). The FireMapper thermal-imaging radiometer has been designed to measure the very high infrared radiances of wildland fires (Riggan and Hoffman 2003) and is the only such system widely applied in fire research today. FireMapper has been deployed to multiple large fires during the 2003, 2006, 2007, and 2008 fire emergencies in California and often at times when fires were most active and high-value resources and communities were threatened (Figures 1 and 2). FireMapper data allow

quantitative measurements of fire-spread rates; fire temperatures, radiant-energy flux, and residence time; and fire-line geometry. Image products are made available at www.fireimaging.com, in near-real time, for use by incident management teams.

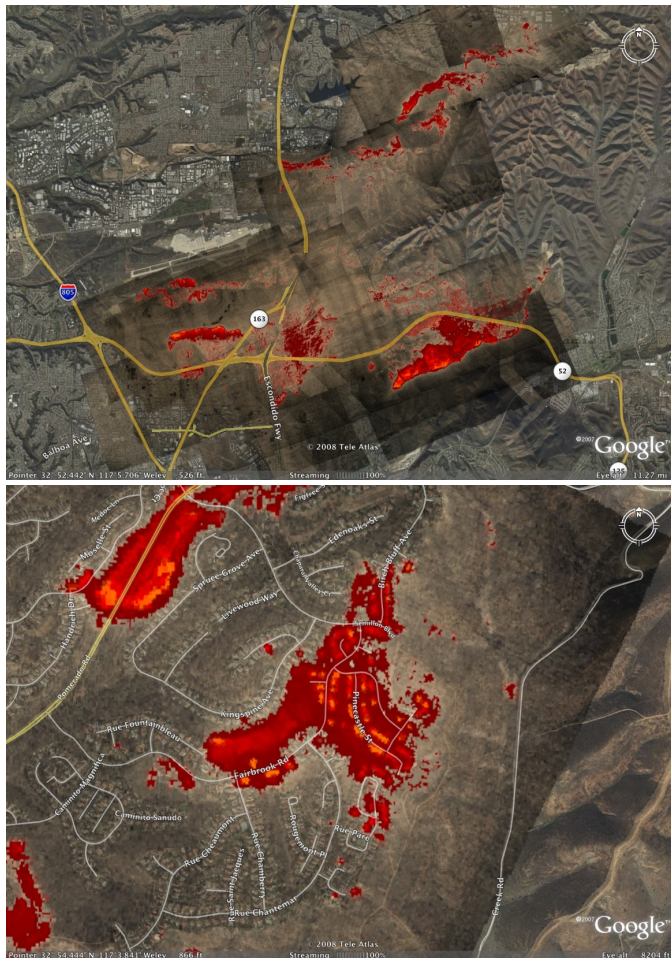


Figure 1. Western portion of the Cedar Fire, San Diego County, California, as viewed from above by the PSW FireMapper, 26 October 2003. Color-coded surface temperatures, which reflect fire radiant-energy flux or intensity, are shown as posted as a Google Earth overlay at www.fireimaging.com. Here a Santa Ana wind is driving the fire to the west-southwest through chaparral and light fuels and across major freeways into portions of the City of San Diego (top image). Higher temperature objects at center of the detail from the vicinity of Pinecastle Street (lower image) are burning homes.

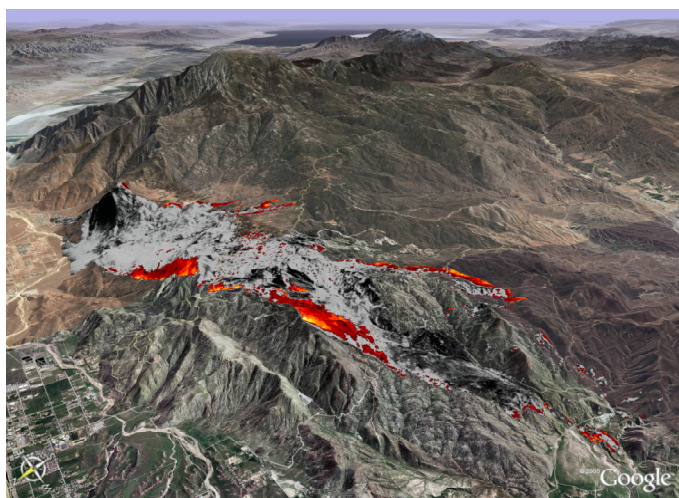


Figure 2. Esperanza Fire, Riverside County, California, as first viewed from the northwest by the PSW FireMapper, 26 October 2006. Here a moderate Santa Ana wind is driving the fire to the southwest through chaparral and light fuels along the northwest flank of Mt. San Jacinto. Note the high temperatures and long residence time in heavy fuels at the center of the northern flank of the fire and the low values in light fuels at the fire's head (lower right).

The FireMapper system is now flown by PSW aboard Forest Service aircraft N127Z, an A100 King Air, which is operated in conjunction with the Forest Health Technology Enterprise Team. Incident management teams in California may order the FireMapper through the Southern Operations Coordination Center.

The PSW FireMapper system incorporates infrared cameras operated at one short-wave (1.6 μm), one mid-wave (3.9 μm), and two long-wave or thermal-infrared wavelengths (at 8.5 and 11.9 μm). Direct observations and modeling of fire radiances show that the radiance measured in the short-wave infrared primarily arises from emissions by very hot but optically thin flames within a fire front; those measured in the thermal infrared (at 11.9 μm) arise from the hot but lower temperature (and high emissivity) ground surface, even beneath active flames (Riggan and Tissell 2009). Both sources, flames and the hot ground surface, contribute strongly to the fire radiance measured at the mid-wave infrared wavelength. Fire radiance measurements at 1.6- and 3.9- μm wavelength have been combined to estimate flame properties including their temperature, combined emissivity and fractional area within a viewing pixel, and radiant-flux density – the rate of radiant energy release per area of ground and per second (see, for example, Riggan *et al.* 2004, Riggan and Tissell 2009). Furthermore, fire temperature and emissivity-fractional area have been correlated with heat and carbon fluxes from large fires and may be used to estimate rates of fuel consumption (Riggan *et al.* 2004).

FireMapper images are of high resolution: the thermal imager employs 1.8-milliradian optics, with a resulting pixel spacing of 1.8 m per 1000 m above ground level. A typical flight at 17,500 feet over 5,000-foot terrain would produce imagery of 6.9-m resolution at nadir.

In support of fire operations, we have disseminated fire-temperature maps derived from the long-wave infrared as measured by the FireMapper. These color-coded image mosaics depict current and recent behavior by active fires: very-high surface temperatures are typically associated with active and intense flaming combustion in heavy fuels; wide reaches of ground with elevated temperatures behind a fire front reflect recent fire movement through relatively heavy fuels (Figure 2). Lower temperatures behind a fire front represent mixtures of small amounts of residual flaming combustion and cooling of the hot ground surface. In our scheme, we typically display progressive temperatures above residual heat from the fire in progressive colors of red, orange, and yellow. Black ash in the sun may be as warm as 75°C; we currently display surface temperatures below that point in shades of tan and gray.

Thermal-infrared imagery has also proven useful in tracking aerial applications of fire retardant; areas recently treated may be as much as 10°C cooler than the surroundings. Successive mapping of fire lines will show new applications and provide an opportunity to assess a measure of both the continuity and apparent density of retardant applications and the response of the fire to the application (Figure 3).

FireMapper imagery is georeferenced, orthorectified, and disseminated in several map products including geoTIFF images, .kmz files for use in Google Earth, in a Google Maps viewer, and as shape files for incorporation in incident-team GIS databases. A Flash-based viewer at fireimaging.com allows an online user to zoom and pan fire imagery and record the latitude and longitude of selected points. This feature can be used to digitize a fire perimeter or record the location of critical fire activity, such as spot fires that have crossed a fire line, road, or natural barrier.

Although the behavior of active fires can be readily tracked by repeated flights with the FireMapper, both short-term prediction or extrapolation of fire behavior on time scales from hours to days and an understanding of why a fire evolves in a given pattern require highly

resolved information on fuels and wind across landscapes. We have applied the Coupled Atmosphere Wildland Fire Environment simulation model (CAWFE) (Coen 2005) to understand atmospheric motions in terrain and interactions of fire with the atmosphere (Coen and Riggan 2010). Yet at present even such sophisticated modeling relies on the basic Rothermel formulation for fire spread and very coarse estimates of chaparral fuels.

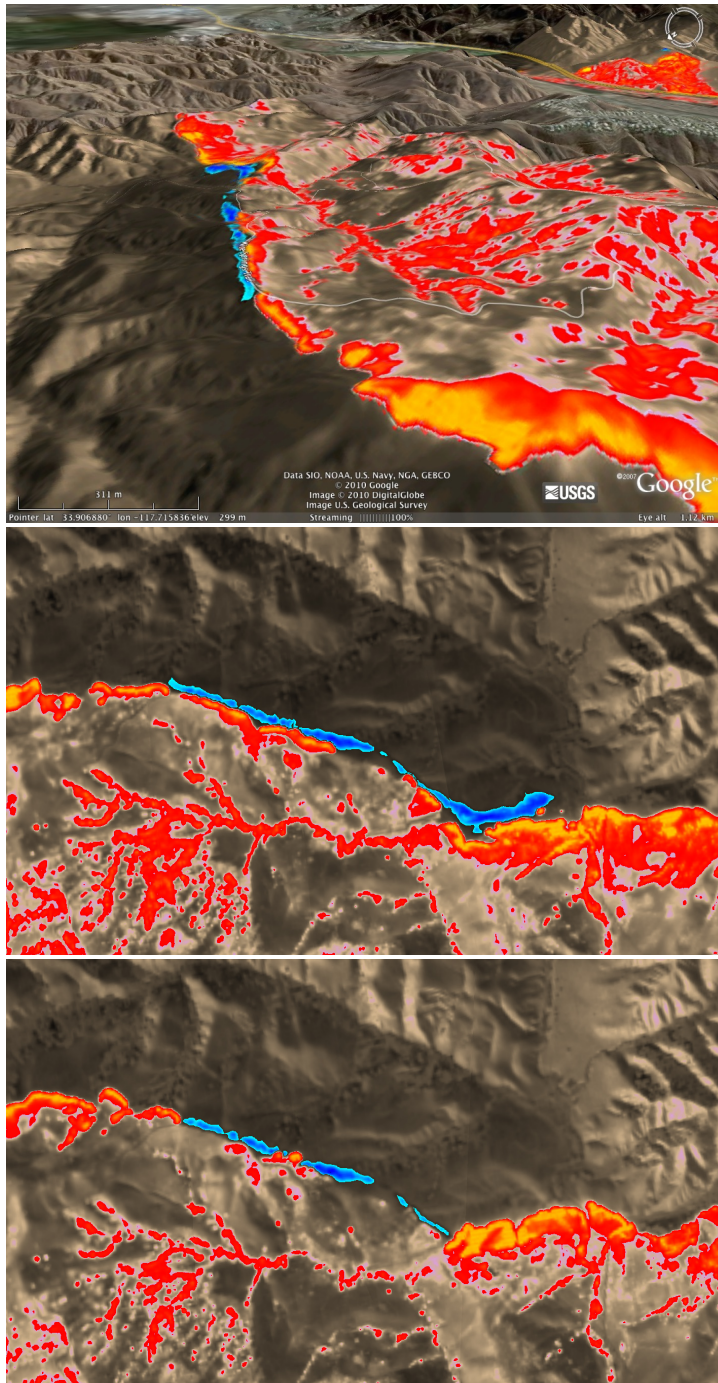


Figure 3. Freeway Fire, 15 November 2008, as viewed by the PSW FireMapper. Here a Santa Ana wind is driving the fire west in grass and chaparral north of the 91 Freeway in Orange County, California. Fire temperatures are color-coded as in Figure 1 (with a tan-to-red transition at 60°C).

Recently applied fire retardant is shown in shades of blue according to the degree of depression in surface temperatures. In the upper image is a view from the northwest, showing the alignment of the retardant along a ridge trending east to west. A nadir view at 14:02 Pacific Standard Time (center image, oriented with north at top) shows small apparent discontinuities in the applied retardant. A nadir view at 14:32 (lower image) shows that the fire was indeed impeded along a portion of the retardant line on the west, burned across the retardant in heavy fuels at the east, and breached the retardant at west-center. Ultimately the line alone was ineffective as the fire spread around the east end of the retardant line and continued into the City of Yorba Linda on the west.

Mapping fuels

Fuel properties are now commonly specified, for example by the LANDFIRE project (data *available online*²), using fuel models such as reported by Anderson (1982) or Scott and Burgan (2005). These models neither describe fuel development with time nor encompass the wide range of extant fuel conditions in chaparral. Fuel model 4, as reported by Anderson, was one of several models devised for fire-danger rating (Rothermel 1972). It has been widely and uncritically applied to chaparral (and is recommended as well for pocosin and southern rough). Fuel model 5 has been assumed as a description for younger chaparral with little dead fuel. We have been unable to discover the provenance of these models. Scott and Burgan (2005) specify four models for dry-climate shrub lands, two of which are appropriate for chaparral. Thus the available mapping data show primarily where there is chaparral fuel, but little about its variability. A photo-series guide to chaparral fuels (Ottmar *et al.* 2000) provides tables of measured loadings by size class and condition (dead or live) for 16 stands of chaparral and coastal sage scrub, with the intent that a user can visually compare a stand in the field with photos in the guide to select rough estimates of fuels. The procedure is useful but neither constitutes a measurement nor provides a means to estimate fuel distribution across landscapes or development with time. We note that in a few instances Scott and Burgan have obtained photos from Ottmar *et al.* to illustrate examples for their fuel models, but do not explicitly use the tabled fuel data from Ottmar *et al.*

Chaparral stand development

As with forest ecosystems, productivity and biomass accumulation in chaparral exhibit a wide natural range (Figure 4) and are strongly affected by site quality or environment, community type, and possibly by stand density. The greatest rates of primary production at the San Dimas Experimental Forest (SDEF) in Los Angeles County rival those of the eastern deciduous forest (Riggan *et al.* 1988). For mature chaparral stands, say, near 20 years of age, total aboveground biomass may range from 2 to 12 kg/m²! Variation across age must be even greater. Thus, a few stylized fuel models must be woefully inadequate to describe the range of biomass accumulation in chaparral.

Growth in chaparral is most limited by availability of water (or water stress), extremes of temperature, and possibly nitrogen or phosphorus availability (cf. Mooney *et al.* 1975, Oechel and Hastings 1983). Greatest rates of biomass accumulation have been recorded in *Ceanothus* chaparral in the San Gabriel and Santa Ynez Mts., and especially, on north-facing aspects (Riggan *et al.* 1988, Schlesinger and Gill 1980). Foliage biomass on a presumably mesic north-facing slope at a site in San Diego County was shown to be three times greater than on an adjacent, xeric, south-facing aspect, although soil moisture was seasonally depleted slightly more quickly on the northern aspect (Ng and Miller 1980). Leaf area on these sites apparently was adjusted during stand development to optimize water-use efficiency. Foliage mass in *Ceanothus* continues to accumulate at least through age 22 years, although the rate of accumulation begins to decline at around age 14 years (Riggan *et al.* 1988). The rate of total aboveground biomass accumulation shows no such decline prior to age 22.

Biomass accumulation during stand development has been approached by measurement of similar sites across age-class boundaries (e.g., by Schlesinger and Gill 1980) and by reconstruction of biomass accumulation for individual stands (e.g., by Riggan *et al.* 1988). These approaches are useful in providing expected trends in fuel properties with vegetation age.

² <www.landfire.gov>

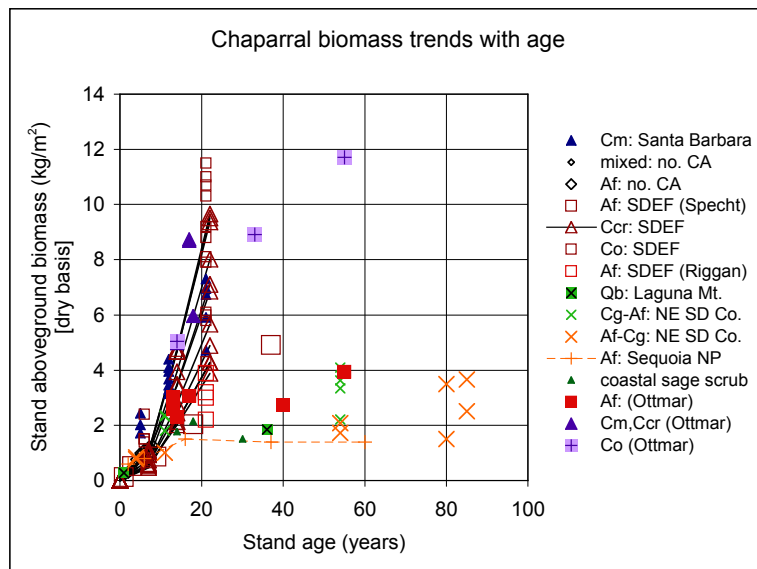


Figure 4. Trends in chaparral biomass with age (adapted from Riggan *et al.* 1994). Aboveground biomass reflects a wide range of primary production across complex environments and community types in chaparral. Data are from Ottmar *et al.* (2000) and sources provided in Riggan *et al.* (1994). Identified species are Af: *Adenostoma fasciculatum*, Ccr: *Ceanothus crassifolius*, Cg: *C. greggii*, Cm: *C. megacarpus*, Co: *C. oliganthus*, Qb: *Quercus berberidifolia*.

Biomass as fuel

Not all chaparral biomass is likely to be consumed during burning. One expects a chaparral fire in stands of intermediate age to consume all foliage and deadwood, finer fractions of live wood, and dry leaf litter. Nine percent of live woody biomass was consumed by each of two prescribed fires of differing activity in 26- and 27-year-old chaparral at the SDEF (Riggan *et al.* 1994), yet stand age and associated fuel loading and condition apparently are important: For example, the 1985 Sherwood Fire in Los Angeles County produced a mosaic of burned and unburned vegetation and consumed foliage and only the finest of woody twigs, spreading in part through *Salvia mellifera* [black sage] and grass fuel in 8-year-old *Adenostoma fasciculatum* [chamise] and *C. megacarpus* chaparral. A black ash surface remained in burned areas. Concurrent burning in 50-year-old chaparral there was of exceptionally high-intensity as all foliage, fine wood, leaf litter, and many live stems 5- to 10-cm in diameter were incinerated. Virtually no unburned vegetation remained within the fire perimeter in this age class, and the ground surface was uniformly covered with a deep white ash (Riggan *et al.* 1994). Thus an understanding of fuel requires both estimates of biomass accumulation and the proportion of the biomass that is consumed, and the latter probably changes with stand age or condition or fire intensity.

As chaparral stands age, deadwood accumulates through progressive shading (or aging) of lower branches, declines or dieback induced by extreme drought or pathogens, intra- or inter-specific competition, and random mortality such as that from snow or freezing (Riggan *et al.* 1994). The median deadwood fraction in chamise across 15 sites in southern California has been reported to be 0.23 (Paysen and Cohen 1990). Yet chamise has been observed to accumulate little deadwood in low productivity environments (0.07 of aboveground biomass) and a substantial fraction (0.45 to 0.48) in high-productivity stands where it is subject to competition from tall *Ceanothus* (Riggan *et al.* 1988). Note that although the *fraction* of biomass that is deadwood may not change substantially with age, biomass accumulation with aging would indeed lead to higher deadwood loadings. Some mortality may be rapid and episodic: A drought-related dieback in *C. crassifolius* at the SDEF was shown to kill 0.38 of the aboveground biomass within a few months in 1985 (Riggan *et al.* 1994). We also observed some

stands of *C. oliganthus* on north-facing aspects that had suffered almost complete mortality at about the same time.

By reference to controlled fires in the laboratory, the behavior of spreading chaparral fires also may depend on the physical arrangement of the fuel, especially the ratio of surface area to volume of fuel elements and the physical packing of the fuel, i.e., its volume fraction within the shrub canopy. Such fuel properties have rarely been measured or estimated for chaparral; Countryman and Philpot (1970) did so for a limited sample of 16 chamise shrubs from a single location at the North Mountain Experimental Area in Riverside County. Because the chaparral plant canopy carries a fire, effects of changes in bulk density with stand age are probably most important in that canopy; such changes with age are not well known. In 21-year-old *C. crassifolius* at the SDEF, ca. three-quarters of the foliage mass was located between 2 and 4 meters of the ground surface with one-tenth of the foliage above that height in stands averaging 4 m height (Riggan et al. 1988).

We envision that useful fire-behavior prediction in southern California will ultimately require landscape-level models of stand biomass accumulation as a function of environment and age with links to remote-sensing measurements of plant-community type, and plant-canopy development. *It may also be possible to directly relate remote sensing measurements of fire properties to prefire vegetation reflectance properties.* As an example of the latter concept, we note that the maximum temperatures observed along a fire line in chaparral often show a spatial correspondence with changes in apparent vegetation density as associated with different landscape aspects (Figure 5).

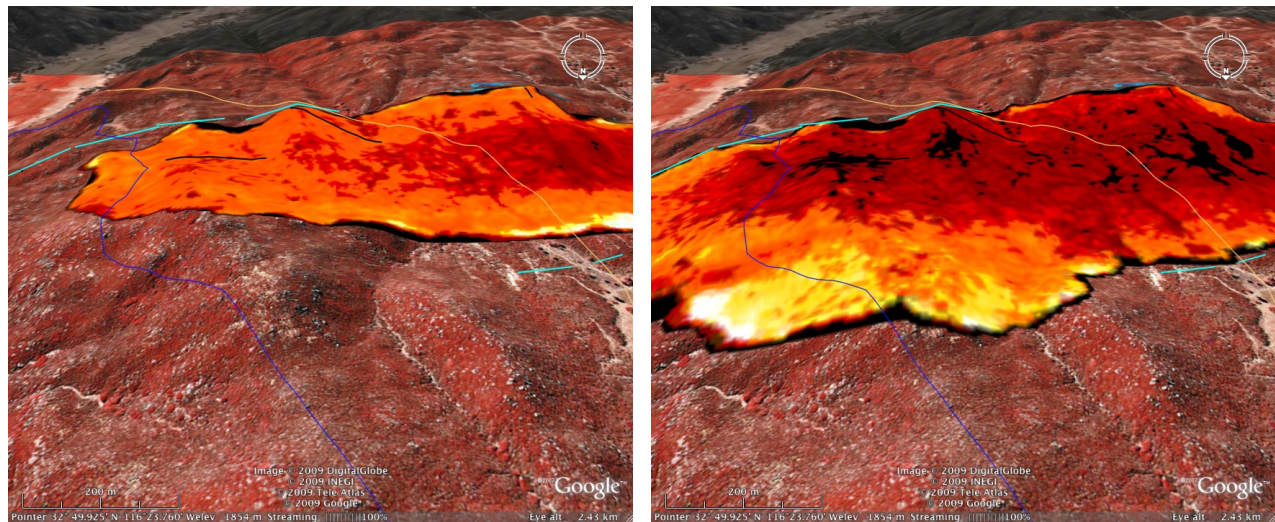


Figure 5. Troy Fire, San Diego County, California as viewed from the north by the FireMapper thermal imaging radiometer, 19 June 2002, at 14:06 (left) and 14:53 (right) Pacific Daylight Time. Note that the maximum temperatures associated with the fire front (yellow and white tones) were greatly elevated when fire spread into chaparral on more northerly-facing aspects as indicated by the base false-color infrared photography.

Estimating fuels at the Esperanza Fire

To examine the use of multispectral remote sensing as an estimator of fuel properties, we have estimated chaparral fuel loading and likely consumption in the area of and surrounding the 2006 Esperanza Fire in Riverside County. Chaparral biomass was estimated from a combination of

(1) post-fire measurement of the basal area of remaining shrub stems from 127, circular, 1/250-acre plots (D. Weise, *personal communication*) that were distributed in the area of active fire runs as observed by remote sensing with the FireMapper, (2) scaling relationships of biomass components to basal area for shrubs prior to burning and at different ages and for several species, and (3) correlation of pre-fire stand biomass estimates to broader averages of vegetation reflectance derived from Landsat Thematic Mapper (TM) imagery. Relations of prefire biomass components to stem basal area were obtained from measurements in the vicinity of the Esperanza Fire by C. Wright (*personal communication*) and earlier measurements in 55-year-old chaparral there by J. Regelbrugge (*U.S. Forest Service records on file, Riverside, CA*). Stand biomass estimates followed the approach previously described, for example, by Riggan *et al.* (1988), Schlesinger and Gill (1980), and Conard and Regelbrugge (1993).

The fine live biomass (B_f) estimated for Weise's 4.6-meter-diameter field plots showed, on a plot by plot basis, little correspondence to prefire estimates of the normalized difference vegetation index (NDVI), defined as $(nIR-red)/(nIR+red)$ reflectances, as determined from 30-m TM data collected in either February or June 2006. However, averaging plot biomass and NDVI values by four ranges of ages and north and south aspects produced a good relationship between the variables with a power function regression accounting for 0.80 of the variance in $\ln(B_f)$ (Figure 6a). Apparently, large differences in scale and uncertainty in location between the small field plots and much larger TM pixels obscured a large-scale relationship between the reflectance and vegetation measurements. Available data also showed that the ratio of fine live woody biomass to foliage biomass was very similar between 10- and 55-year-old stands, and deadwood biomass was similar and low in young *Arctostaphylos glandulosa* [manzanita] and chamise but substantially higher at age 55 years for either species (Figure 6b). Accordingly, we fit a power function to these latter data so as to reasonably interpolate the rate of dead biomass accumulation with age.

The results of this analysis (Figures 7 to 12) show a range of fuel loading associated with elevation and stand age that was not captured by application of the standard fuel models. The loading showed a general correspondence with observed fire behavior, specifically, the low energy release rates behind the main fire front in light fuels as shown in Figure 2, high energy release on north-facing slopes, as along the north side of Mt. Edna, and high energy release associated with narrow reaches of old chaparral in the southwest of the fire adjacent to Poppet Flat (Figure 11). The Esperanza Fire terminated in the southwest coincident with the boundaries of earlier fires and young fuels. Spatial discontinuities in surface temperatures after passage of the fire front were also noted to coincide with age-class boundaries. The Landsat NDVI measure showed skill in predicting broad classes of fuel accumulation and fire properties, yet sampling limitations precluded a more detailed analysis based on stand species composition and led to extrapolations at higher apparent biomass loading at higher elevations and low fuel loading in frequently burned and degraded landscapes.

Concluding remarks

Airborne remote sensing with the FireMapper thermal-imaging radiometer is providing unprecedented information on the short-term behavior and energetics of wildland fires in southern California. Extending fire measurements with predictive models will require extension of operational fire-behavior models to the extreme conditions of energy release of large wildland fires in chaparral and substantial improvements in measurement and modeling of chaparral fuel development with age and environment and rates of fuel consumption. Measurements of

biomass in the field and by multispectral remote sensing have been combined to estimate fuel loading for the 2006 Esperanza Fire and these data are providing inputs for simulations with coupled fire-atmospheric dynamics models including NCAR's CAWFE model. We recommend extending this approach by applying fuel sampling and multispectral remote sensing across a wider range of environments and rates of chaparral productivity. Resulting fuel estimation models should then be combined with climatology and remote measurements of available moisture to model and map stand fuel development with age in important chaparral and grass fuel types in southern California. Measurements should characterize the ratio of foliage surface area to volume and trends with stand age in the development and vertical structure of foliage and fine live woody biomass, accumulation of live and deadwood by size class, and fuel-bed packing ratio. Modeled fuel and fire properties should then be independently evaluated against remotely sensed behavior of large wildland fires.

Resulting improvements in fuel and fire-behavior models will support tactical fire suppression by providing a basis to evaluate expected fire behavior and support strategic fuel management by allowing an evaluation of regional fire risk and the response of wildland fires to extant fuel condition and potential fuel treatments.

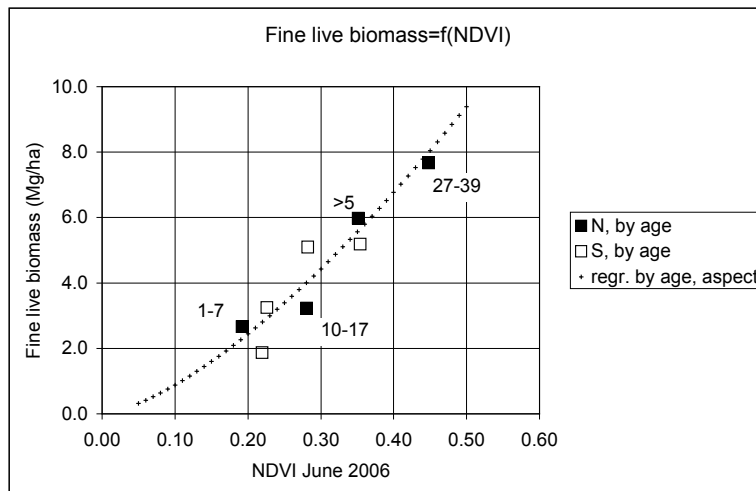


Figure 6a. Relation of average fine live biomass (B_f) to NDVI for groupings of field measurements by categories of age and aspect at the 2006 Esperanza Fire. Age categories (in years) are labeled for the average values associated with north-facing aspects. A power-function model, $B_f = 26.0(\text{NDVI})^{1.47}$, estimated by regression of the average values is shown (+ symbols).

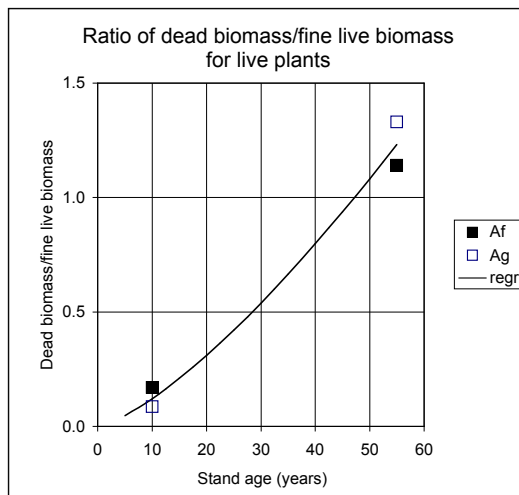


Figure 6b. Changes with stand age in the ratio of deadwood biomass to fine live biomass for two chaparral species: *Adenostoma fasciculatum* (Af) and *Arctostaphylos glandulosa* (Ag). Data were collected from within the perimeter of the Esperanza Fire (C. Wright personal communication, J. Regelbrugge U.S. Forest Service data on file, Riverside, CA). A power function model was used here to interpolate by age.

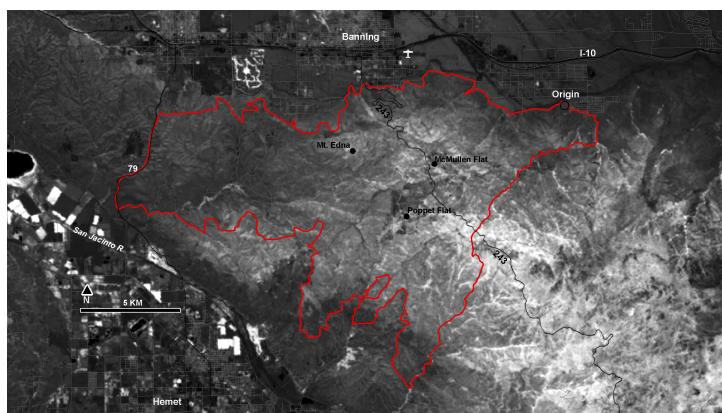


Figure 7. Normalized Difference Vegetative Index mapped in the vicinity of the 2006 Esperanza Fire from pre-fire LANDSAT TM data, imaged in June 2006. All values in the area of interest are positive: scaling is such that an NDVI value of zero is mapped to black; a value of one is mapped to white. The fire perimeter is shown in red.

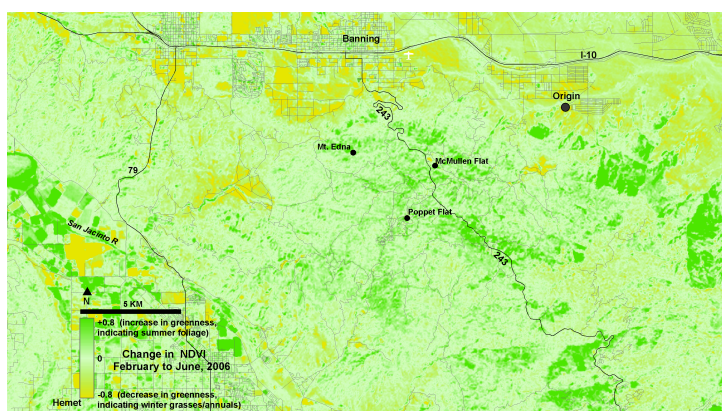


Figure 8. Difference image of Normalized Difference Vegetative Index values between June and February 2006. Negative difference values, where values from February are greater than in June (assigned yellow tones) correspond to annual grasslands and herbaceous vegetation. Higher positive values (assigned deeper green tones) correspond to developing foliage in shrubs and woodlands.

Acknowledgments

The authors thank Robert Lockwood and James Brass for reviews of this manuscript and Clint Wright for making available stand structure and biomass data from the Esperanza Fire. Trade names, commercial products, and enterprises are mentioned solely for information. No endorsement by the U.S. Department of Agriculture is implied. This material is partly based upon work supported by the National Fire Plan and the Joint Fire Science Program and by the National Science Foundation under Grants No. 0324910, 0421498, and 0835598. The National Center for Atmospheric Research is sponsored by the National Science Foundation. Any opinions, findings, and conclusions or recommendations expressed in this material are those of the authors and do not necessarily reflect the views of the National Science Foundation.

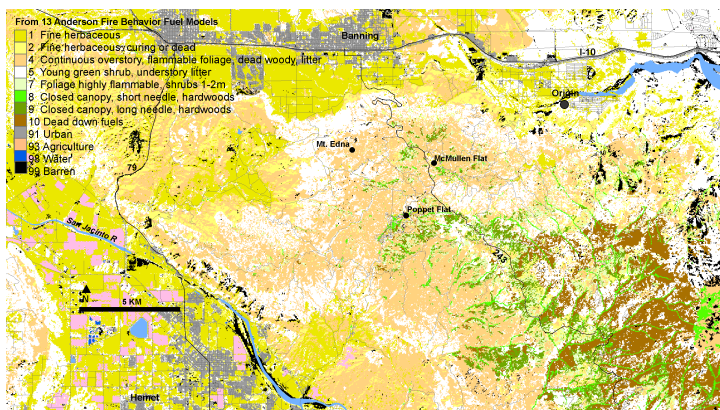


Figure 9. LANDFIRE fuel models in the vicinity of the 2006 Esperanza Fire. The majority of the fire area falls into two classes of chaparral creating essentially a binary model for fuels: high and low.

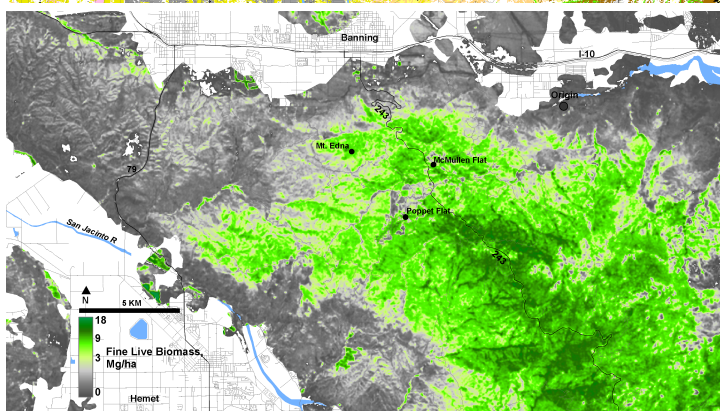


Figure 10. Mapped fine live biomass (0-1/4" wood plus foliage) in the vicinity of the 2006 Esperanza Fire, as estimated from NDVI (Figure 7) and the relation of B_f to NDVI (Figure 6a). Highest values (dark green) are outside of the fire perimeter; together with the lowest values in grass and herbaceous types (darker grays), these constitute an extrapolation from available data based on chaparral.

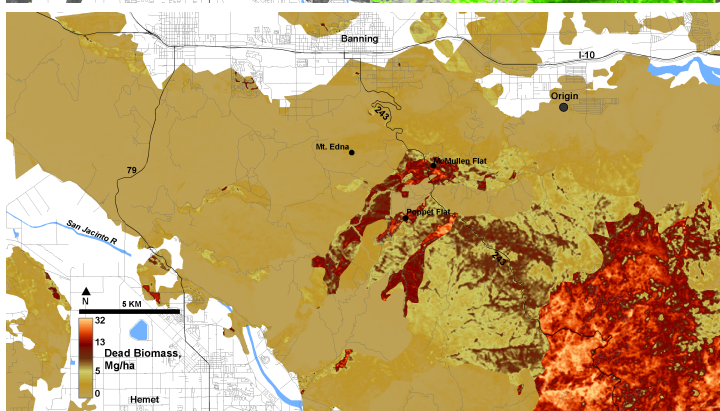


Figure 11. Mapped deadwood-fuel loading for the area shown in Figure 10. Values are derived as a fraction of fine live biomass that varies with stand age (Figure 6b). Highest values in the southeast are outside of the fire perimeter and correspond to more productive chaparral and oak woodlands with some conifers and no fire history. Strips of high deadwood loading at center correspond to high-intensity fire runs as observed with the FireMapper.

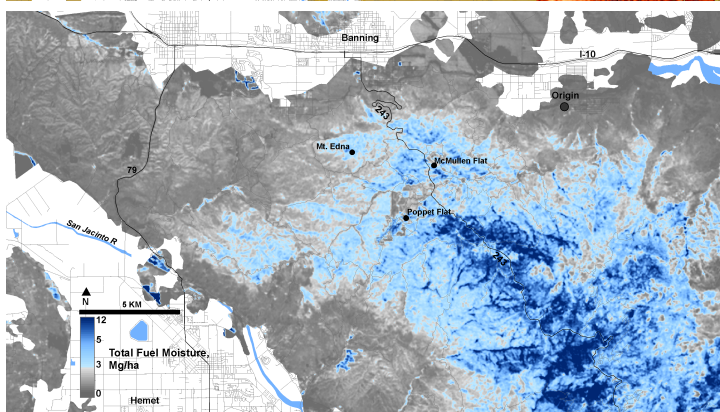


Figure 12. Estimated moisture in fine live wood, foliage, and deadwood for the area of the Esperanza Fire. The latent heat of vaporization associated with this moisture will reduce the energy available to propagate the fire.

References

- Anderson HE (1982) Aids to determining fuel models for estimating fire behavior. USDA Forest Service, Intermountain Forest and Range Experiment Station General Technical Report INT-122. (Ogden, UT)
- Coen JL (2005) Simulation of the Big Elk Fire using coupled atmosphere-fire modeling. *International Journal of Wildland Fire* **14**, 49–59.
- Coen J, Riggan PJ (2010) A landscape-scale wildland fire study using a coupled weather-wildland fire model and airborne remote sensing. Proceedings of the 3rd Fire Behavior and Fuels Conference, October 25-29, 2010, Spokane, Washington, USA. (International Association of Wildland Fire: Birmingham, AL)
- Conard SG, Regelbrugge JC (1993) On estimating fuel characteristics in California chaparral, pp. 120-129, In: Proceedings of the 12th Conference on Fire and Forest Meteorology, October 26-28, 1993, Jekyll Island, Georgia. (Society of American Foresters: Bethesda, MD)
- Countryman CM, Philpot CW (1970) Physical characteristics of chamise as a wildland fuel. USDA Forest Service, Pacific Southwest Forest and Range Experiment Station Research Paper PSW-66. (Berkeley, CA)
- Fendell FE, Carrier GF, Wolff MF (1990) Wind-aided firespread across arrays of discrete fuel elements. Defense Nuclear Agency Technical Report DNA-TR-89-193. (Alexandria, VA)
- Franklin J, Spears-Lebrun LA, Deutschman DH, and Marsden K (2006) Impact of a high-intensity fire on mixed evergreen and mixed conifer forests in the Peninsular Ranges of southern California, USA. *Forest Ecology and Management* **235**, 18-29.
- Los Angeles Times. October 25, 2007. 1 million fled fires? As the smoke clears, the estimates shrink. Available online: http://www.latimes.com/news/local/la-me-evacuation25oct25_0,6746893.story.
- Mooney HA, Harrison AT, Morrow PA (1975) Environmental limitations on photosynthesis of a California evergreen shrub. *Oecologia* **19**, 293-301.
- National Wildfire Coordinating Group (2009) Historical Incident ICS-209 Reports. Available online at: http://fam.nwcg.gov/fam-web/hist_209/report_list_209.
- Ng E, Miller PC (1980) Soil moisture relations in the southern California chaparral. *Ecology* **61**(1), 98-107.
- Oechel WC, Hastings SJ (1983) The effects of fire on photosynthesis in chaparral resprouts. In: Mediterranean Type Ecosystems: The Role of Nutrients. (Eds. FJ Kruger, DT Mitchell, UM Jarvis) pp. 274-285. (Springer-Verlag: New York)
- Ottmar RD, Vihnanek RE, Regelbrugge JC (2000) Stereo photo series for quantifying natural fuels. Volume IV: pinyon-juniper, sagebrush, and chaparral types in the Southwestern United States. National Wildfire Coordinating Group, National Interagency Fire Center PMS 833. (Boise, ID)
- Paysen TE, Cohen JD (1990) Chamise chaparral dead fuel fraction is not reliably predicted by age. *Western Journal of Applied Forestry* **5**(4), 127-131.
- Riggan PJ, Franklin SE, Brass JA, Brooks FE (1994) Perspectives on fire management in Mediterranean ecosystems of southern California. In: Fire and global change in Mediterranean Ecosystems. (Eds. J Moreno, W Oechel) pp. 140-162. Ecological Studies 107. (Springer-Verlag: New York).
- Riggan PJ, Goode S, Jacks PM, Lockwood RN (1988) Interaction of fire and community development in chaparral of southern California. *Ecological Monographs* **58**(3), 155-176.

- Riggan PJ, Hoffman JW (2003) FireMapper: a thermal-imaging radiometer for wildfire research and operations. *Proceedings of the IEEE Aerospace Conference*, Big Sky, MT, paper 1522.
- Riggan PJ, Lockwood RN, Tissell RG, Brass JA, Pereira JAR, Miranda HS, Miranda AC, Campos T, Higgins R (2004) Remote measurement of wildfire energy and carbon flux from wildfires in Brazil. *Ecological Applications* **14**(3), 855-872.
- Riggan PJ, Tissell RG (2009) Airborne Remote Sensing of Wildland Fires. In: Wildland Fires and Air Pollution. (Eds. A Bytnerowicz, M Arbaugh, A Riebau, C Andersen) pp. 139-168. *Developments in Environmental Science* 8. (Elsevier Publishers: Amsterdam, The Netherlands)
- Rothermel RC (1972) A mathematical model for predicting fire spread in wildland fuels. USDA Forest Service, Intermountain Forest and Range Experiment Station Research Paper INT-115. (Ogden, UT)
- Schlesinger WH, Gill DS (1980) Biomass, production, and changes in the availability of light, water, and nutrients during the development of pure stands of the chaparral shrub, *Ceanothus megacarpus*, after fire. *Ecology* **61**(14), 781-789.
- Scott JH, Burgan RE (2005) Standard fire behavior fuel models: a comprehensive set for use with Rothermel's surface fire spread model. USDA Forest Service, Rocky Mountain Research Station General Technical Report RMRS-GTR-153. (Fort Collins, CO)